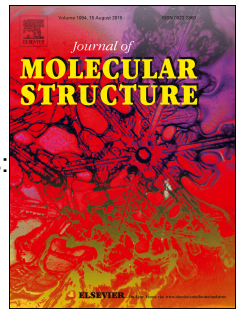

Design, crystal structures and sustainable synthesis of family of antipyrine derivatives: Abolish to bacterial and parasitic infection

Gurjaspreet Singh, Pinky Satija, Baljinder Singh, Shweta Sinha, Rakesh Sehgal, Subash Chandra Sahoo

PII: S0022-2860(19)31110-X

DOI: https://doi.org/10.1016/j.molstruc.2019.127010

Reference: MOLSTR 127010

To appear in: *Journal of Molecular Structure*

Received Date: 18 July 2019

Revised Date: 30 August 2019

Accepted Date: 31 August 2019

Please cite this article as: G. Singh, P. Satija, B. Singh, S. Sinha, R. Sehgal, S.C. Sahoo, Design, crystal structures and sustainable synthesis of family of antipyrine derivatives: Abolish to bacterial and parasitic infection, *Journal of Molecular Structure* (2019), doi: https://doi.org/10.1016/j.molstruc.2019.127010.

Design, Crystal Structures and Sustainable Synthesis of family of antipyrine derivatives: Abolish to bacterial and parasitic infection.

Gurjaspreet Singh[a*], Pinky Satija[a], Baljinder Singh[b], Shweta Sinha[c], Rakesh Sehgal[c], Subash Chandra Sahoo[a]

[a] Department of Chemistry, Panjab University, Chandigarh 160014, India.

[b] Department of Biotechnology, Panjab University Chandigarh, 160014, India

[c] Department of Medical Parasitology, PGIMER, Chandigarh-160012, India.

[*]Corresponding Author

Dr. Gurjaspreet Singh

Professor,

Department of Chemistry,

P.U., Chandigarh

India

+91-0172-2534428,

Email: gjpsingh@pu.ac.in

Graphical Abstract

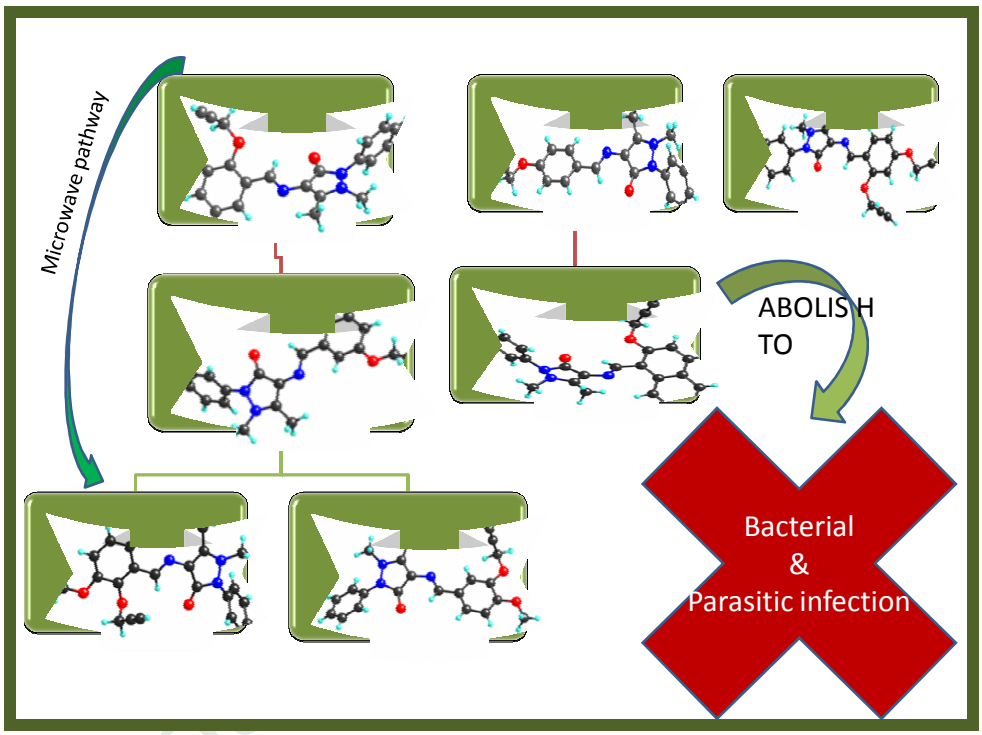

Abstract

This work explores the facile synthesis of a series of antipyrine acetylinic framework (3a-3h). The newly synthesized compounds are recognized by IR, NMR (^{1}H, ^{13}C), X-ray diffraction. This collection played indispensable role in the development of biologically active agents. Our goal is to enable adoption of green chemistry within the pharmaceutical industry for the benefit of society, industry and the environment. This work articulates a new possible scaffold for drug discovery against protozoal pathogens (Entamoeba histolytica and Giardia lamblia) and bacterial strain (Staphylococcus aureus, Vibrio cholera, E.coli, Bacillus subtillus). The purpose of the present undertaking is to put low price anti parasitic drug using green technology. It is envisaged that the alliance of anti pyrine derivative and acetylene framework into a single scaffold boosts the effectiveness of anti bacterial as well as anti-parasitic treatment and may be vital for meeting future challenges in medicinal world.

Key words: Anti pyrine, Entamoeba histolytica, Giardia lamblia, Microwave methodology, Acetylene framework

Introduction

The microwave irradiation technique, has been triumphantly making inroads in miscellaneous chemistry laboratories such as solid- state chemistry, nanomaterial synthesis, and organic synthesis [1]. The advantage of this fascinating technology is safe, increased reaction kinetics, energy efficiency, purity and high product yields due to minimized the formation of undesired side- products during the reactions[2].

Antipyrine (AP) was first synthesized by Knorr in 1883 [3]. It has a biological versatile structure due to the presence of tribioactive centers like methyl, N and O groups, which generates interest in the studies of antipyrine derivatives (APDs). 4-Aminoantipyrine (AAP) is a metabolite of aminophenazone and its derivatives exhibit a fascinating array of pharmacological activity imputed to their ability to have non covalent interactions with

various active site in organism [4].This fragment exhibit a resemblance with metamizole, a recognized antipyretic agent, analgesic and anti-inflammatory whose potency is unimpeachable[5,6].

Although there were some recognized reactions grabbing the acetylene framework such as Huisgen 1, 3-dipolar cycloaddition, Sonogashira, the Pauson-Khand and Nicholas reactions, the Bergman, Moore and Myers cyclizations yet pharmacological activity of this framework is not reported much**[7].**

Bacterial fouling and parasitic infections are devastating diseases impacting the human society worldwide and global economy significantly. A frightening statistic shows that these infectious diseases kill more than nine million people every year which is more than any other diseases like Parkinson's disease, HIV/AIDS[8,9]. E. histolytica and G. lamblia, protozoan infection that cause amoebic dysentery and giardiasis, respectively[10-12].This usually shows broad range of symptoms such as dysentery, bloating, stomachache, cramps[13, 14].

Bacteria can be categorized into two type: Gram positive and Gram negative that depend on their cell wall structure. The infections due to bacteria may cause severe diseases such as osteomyelitis, endocarditis, and toxic shock syndrome. The problem of antimicrobial resistance is due to insufficiency of investment of the pharmaceutical industry[15] and advanced therapeutic agents.

Nitroimidazole and its derivatives (Fig 1) are the most effective antiamoebic medication, but have several adverse effects including gastrointestinal disturbance, especially nausea, vomiting [16]. Hence, in severe infection it carried out with antimicrobial drugs.

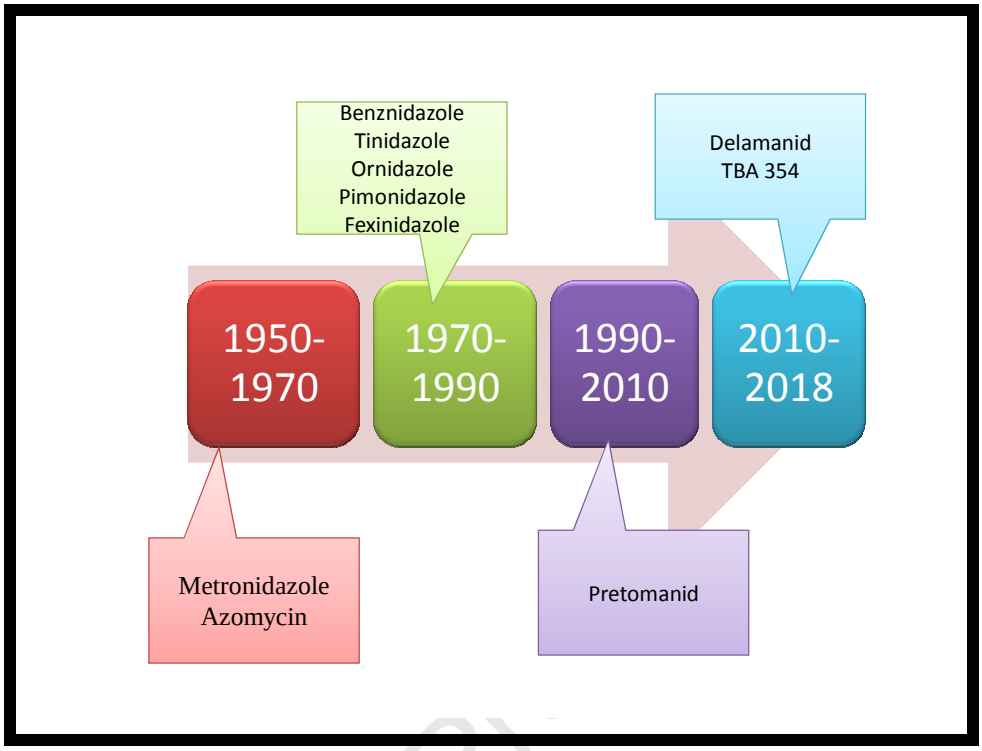

Fig 1: Timeline for the discovery of nitro-imidazole anti-infective agents

The general mechanism of action of nitro imidazole derivatives (Fig 1), involves the formation of reactive nitro radical anion that can lead to DNA degradation and cell death. Therefore there is an urgent need of an ideal approach to combat them with a novel action mechanism drug. The proximity of antipyrine derivatives and acetylene framework, a felicitous choice used to develop new antimicrobial agents.

2. Experimental Protocol

2.1. Materials and measurements.

All commercially available chemicals were used as received without further purification and organic solvents were used after distillation. 4 amino antipyrine(Avra) Propargyl bromide (Aldrich), Potassium carbonate(Thomas), 2-hydroxy benzaldehyde (Avra), 3-hydroxy benzaldehyde(Avra), 4-hydroxy benzaldehyde(Avra), 3-Ethoxy-4-hydroxy benzaldehyde), 2-hydroxy-3 methoxy benzaldehyde(Avra), 4-hydroxy 3 methoxy benzaldehyde(Alfa Aesar), 2-hydroxy naphthaldehyde(Alfa Aesar), 2,4 Dihydroxy benzaldehyde(Avra) were used.

2.2. Physical measurements

The infrared spectra were recorded on a Thermo Scientific NICOLET IS50 spectrophotometer. The 1H and 13C NMR spectra were carried out on a JEOL (AL 400 MHz) spectrometer. Microwave synthesis was conducted in Anton Paar Microwave PRO reaction system. Melting points were measured in a Mel Temp II device using sealed capillaries.

2.3 X-ray Structure determination

Crystals were mounted on Hampton cryoloops. All geometric and intensity data for the crystals were collected using a Super-Nova (Mo) X-ray diffractometer equipped with a micro-focus sealed X-ray tube Mo-Kα (λ = 0.71073 Å) X-ray source, and HyPix3000 (CCD plate) detector of with increasing ω (width of 0.3_ per frame) at a scan speed of either 5 or 10 s/frame. The CrysAlisPro software was used for data acquisition, and data extraction. Using Olex2[17], the structure was solved with the SIR2004[18] structure solution program using Direct Methods and refined with the ShelXL[19] refinement package using Least Squares minimisation. All non-hydrogen atoms were refined with anisotropic thermal parameters. Detail crystallographic data and structural refinement parameters are summarized in Table 5, 6 and 7.

2.4 Statistical analysis

2.4.1. Antiparasitic activity

Drug sensitivity was conducted by using MTT (3-(4,5-Dimethylthiazol-2-yl)-2,5-diphenyltetrazolium bromide, a tetrazole) assay for all Compounds. Highest drug concentration in each rows was 100µg/ml and then doubling dilutions of the drug were performed. The plates were incubated at 37°C for 24 hrs and 48hrs. Following incubation at 37°C for 24hr and 48hr, the optical density (OD) was recorded in an ELISA recorder at 570 nm. Each experiment is executed in triplicate sets. IC_{50} value was measured using Graph Pad Prism version 6.

2.4.2. Antibacterial activity

In the broth dilution MIC method, various concentrations of the compounds were inoculated with a standard suspension of test bacteria. Following an overnight incubation at 37 °C, the MIC was determined by observing the lowest concentration of the compounds that would inhibit visible growth of the test bacteria. Growth was calculated photometrically by measuring the optical density (OD) at 600 nm[20].

2.5 General details

Synthesis and characterization

2.5.1. Synthesis

2.5.1.1 Representative procedure for the synthesis of anti pyrine Schiff's base

Antipyrine functionalized Schiff bases (2a-2h) were prepared as condensation of 4 amino antipyrine and various substituted aromatic aldehyde. Yellow crystalline product is obtained after irradiating for five minutes as shown in scheme 1. The product was dried at room temperature.

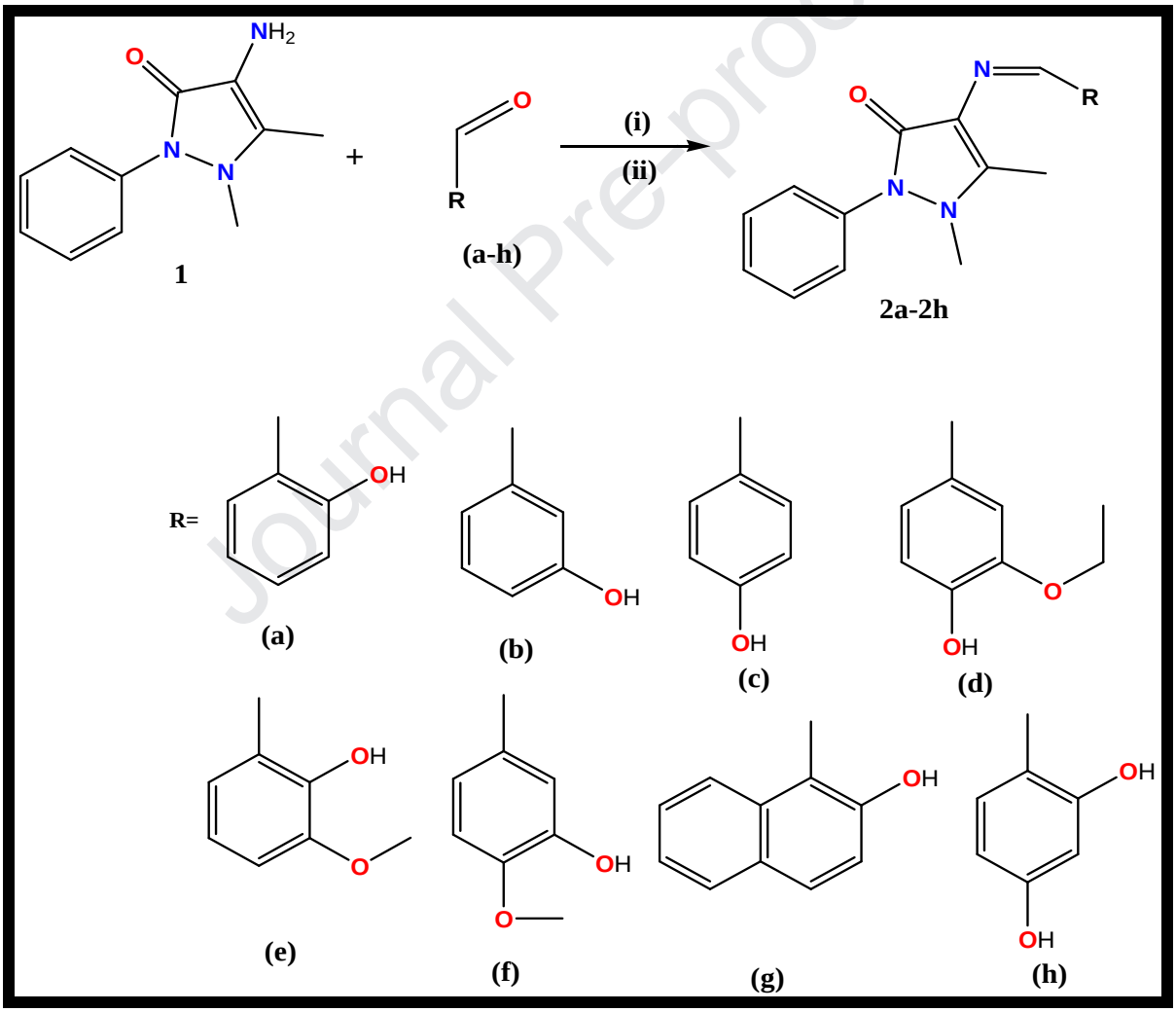

Scheme 1: Synthesis of anti pyrine functionalized Schiff's base (2a-2h). Reagent and Conditions: (i) MW, 5 min, (ii) Ethanol.

Methodology for the synthesis of anti pyrine acetylinic framework

Antipyrine functionalized Schiff bases (2a-2h) were converted into terminal alkynes (3a–3h) (Scheme 2) by using propargyl bromide facilitated by base K_2CO_3 in DMF and the mixture was allowed to age for 16hrs. When the reaction was over, the residue was distilled to recover DMF for the next reaction. After distillation, the residue was poured into cold water, yellow crystalline solid is obtained.

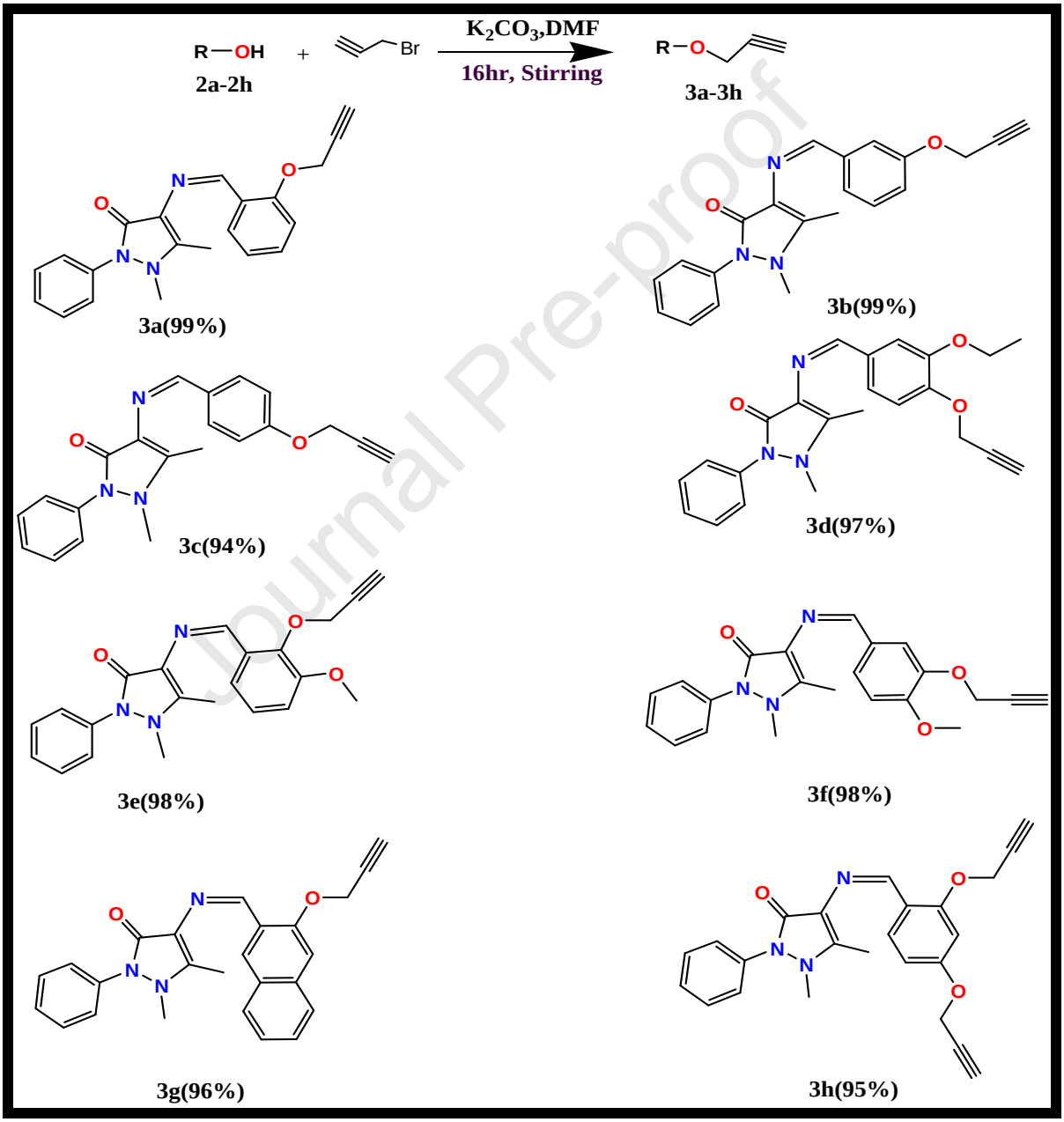

Scheme 2: Synthesis of Anti pyrine functionalized alkynes (3a-3h) using (2a-2h) with% yield.

2.5.2. Characterization:

Synthesis of (3a) 2a (0.32 mmol), propargyl bromide (0.40 mmol).Mustard Crystalline Solid.M.p.:158^{o}C-160^{o}C. IR (cm^{-1}): 3293 (C≡C-H), 3113(N=CH), 2116(C≡C), 1617(C=O), 1603 (C=N), 1413 (CH_3-C), 1270 (CH_2-N), 1168 (O-CH_2), 939 (C-C). 1H NMR (25° C, $CDCl_3$): δ(400 MHz) = 9.73 (s, 1H, CH=N), 7.02–7.85 (m, 9H, Ar), 4.75 (d, 2H,-OCH_2-), 3.15(s, 3H, N-CH_3), 2.57 (t, 1H, -C≡CH), 2.49(s, 3H, C-CH_3).

13C NMR (25^{o}C, $CDCl_3$): δ(101MHz)= 161.0, 159.2, 156.6, 151.7, 134.8, 131.7, 129.2, 129.1, 126.8, 124.2, 118.9, 114.8, 78.2, 75.7, 69.8, 55.8, 35.9, 30.8, 18.8, 10.1.

Synthesis of (3b) 2b (0.32mmol), propargyl bromide (0.40mmol). Yellow Crystalline Solid. M.p.:160^{o}C-162^{o}C. IR (cm^{-1}): 3186 (C≡C-H), 2108(C≡C), 1635 (C=O), 1572(C=N), 1450 (CH_3-C), 1392 (CH_2-N), 1140 (O-CH_2), 959 (C-C).

1H NMR (25^{o}C, $CDCl_3$,): δ(400 MHz)= 9.74 (s, 1H, CH=N), 7.02–8.03 (m, 9H, Ar), 4.76 (d, 2H,-OCH_2-), 3.18(s, 3H, N-CH_3), 2.56 (t, 1H, -C≡CH), 2.51(s, 3H, C-CH_3).

13C NMR (25^{o}C, $CDCl_3$,): δ (101 MHz) = 160.8, 157.9, 157.8, 156.6, 152.1, 139.5, 134.7, 129.5, 129.2, 126.9, 124.4, 121.8, 118.4, 117.3, 112.7, 78.5, 75.6, 55.9, 35.8, 10.1.

Synthesis of (3c) 2c (0.32 mmol), propargyl bromide (0. 40 mmol). Yellow Crystalline Solid. M.p.:170^{o}C-172^{o}C. IR (cm^{-1}): 3288 (C≡C-H), 2108(C≡C), 1625 (C=N), 1454 (CH_3-C), 1384 (CH_2-N), 1172 (O-CH_2), 967 (C-C). 1H NMR (25^{o}C, $CDCl_3$): δ(400 MHz) = 10.10 (s, 1H, CH=N), 7.05–8.18 (m, 9H, Ar), 4.79 (d, 2H,-OCH_2-), 3.16(s, 3H, N-CH_3), 2.51 (t, 1H, -C≡CH), 2.48(s, 3H, C-CH_3).

13C NMR (25^{o}C, $CDCl_3$,): δ(101 MHz)= 160.9, 157.1, 153.2, 152.0, 134.9, 131.1, 129.1, 127.2, 126.7, 126.2, 124.2, 121.4, 119.5, 113.0, 78.6, 75.6, 56.1, 36.0, 10.1.

Synthesis of (3d) 2d (2.84 mmol), propargyl bromide (4.23 mmol).Lemon Coloured Solid(in the form of Fibres).M.p.:174^{o}C-176^{o}C. IR (cm^{-1}): 3240 (C≡C-H), 3182(N=CH), 2116(C≡C), 1635(C=O), 1597 (C=N), 1428 (CH_3-C), 1303 (CH_2-N), 1175, 1215 (O-CH_2), 920(C-C). 1H NMR (25^{o}C,$CDCl_3$): δ(400 MHz)= 9.7 (s, 1H, CH=N), 7.05–7.55 (m, 8H, Ar), 4.83 (d, 2H,-

OCH_2-), 4.21(q, 2H, OC**H**$_2CH_3$), 3.16(s, 3H, N-CH_3), 2.55 (t, 1H, -C≡CH), 2.51(s, 3H, C-CH_3), 1.52(t, 3H, OCH_2C**H**$_3$).

13C NMR (25^{o}C, $CDCl_3$): δ(101MHz) =161.0, 157.0, 151.7, 149.1, 149.0, 134.8, 132.3, 129.1, 126.8, 124.2, 122.1, 118.9, 114.0, 110.6, 78.4, 75.9, 64.3, 56.7, 36.0, 10.2.

Synthesis of (3e) 2e (2.90 mmol), propargyl bromide (3.70 mmol).Yellow crystalline solid. M.p.: 170^{o}C-172^{o}C. IR (cm^{-1}): 3284 (C≡C-H), 2165(C≡C), 1648(C=O), 1571 (C=N), 1470 (CH_3-C), 1372 (CH_2-N), 920 (C-C), 1135, 1268 (O-CH_2).

1H NMR (25^{o}C, $CDCl_3$): δ(400 MHz) = 10.07 (s, 1H, CH=N), 6.69–7.79 (m, 8H, Ar), 4.83 (d, 2H,-OCH_2-), 3.90(s, 3H, -OCH_3), 3.90(s, 3H, N-CH_3), 2.51 (t, 1H, -C≡CH), 2.43(s, 3H, C-CH_3).

13C NMR (25^{o}C, $CDCl_3$): δ(101 MHz) = 160.7, 153.7, 152.9, 152.1, 146.8, 134.9, 132.7, 129.1, 126.7, 124.4, 119.4, 117.8, 113.6, 79.0, 75.9, 60.6, 55.8, 35.9, 10.2.

Synthesis of (3f) 2f (2.90 mmol), propargyl bromide (3.70mmol).Yellow crystalline solid. M.p.: 166^{o}C-168^{o}C. IR (Neat, cm^{-1}): 3287 (C≡C-H), 2136(C≡C), 1648(C=O), 1575 (C=N), 1448 (CH_3-C), 1397 (CH_2-N), 1138, 1258 (O-CH_2), 959 (C-C). 1H NMR (25^{o}C, $CDCl_3$): δ (400 MHz) =9.71 (s, 1H, CH=N), 6.65–7.70 (m, 8H, Ar), 4.86 (d, 2H,-OCH_2-), 3.94(s, 3H, -OCH_3), 3.16(s, 3H, N-CH_3), 2.56 (t, 1H, -C≡CH), 2.51(s, 3H, C-CH_3).

13C NMR ($CDCl_3$, 25^{o}C): δ (101 MHz) = 161.0, 156.7, 151.7, 151.5, 139.5, 134.8, 131.1, 129.1, 126.2, 124.2, 123.5, 118.9, 111.1, 78.3, 75.9, 56.7, 55.9, 36.0, 10.1.

Synthesis of (3g) 2g (3.09 mmol), propargyl bromide (4.80 mmol). Mustard crystalline solid. M.p.: 172^{o}C-174^{o}C. IR (cm^{-1}): 3240 (C≡C-H), 3182(N=CH), 2120(C≡C), 1635(C=O), 1597 (C=N), 1496 (CH_3-C), 1303 (CH_2-N), 1175, 1215 (O-CH_2), 920 (C-C).

1H NMR (25^{o}C, $CDCl_3$): δ(400 MHz) =10.45 (s,1H, -CH=N), 9.49(d, 1H, Naph), 7.28-7.90 (m, 10H, Ar), 4.92 (s, 2H,-OCH_2-), 3.20(s, 3H, -NCH_3), 2.50 (t, 1H, -C≡CH), 2.49(s, 3H, C-CH_3).

13C NMR ($CDCl_3$, 25^{o}C): δ(101 MHz) = 160.8, 156.6, 156.3, 135.0, 131.9, 129.9, 129.1, 128.2, 127.5, 126.7, 126.2, 124.3, 124.2, 120.0, 115.0, 78.8, 75.9, 57.5, 35.9, 10.4.

Synthesis of (3h) 2h(0.390 mmol), propargyl bromide(0. 480 mmol). Pale Yellow Crystalline Solid. M.p.: 170^{o}C-172^{o}C. IR (cm^{-1}): 3265 (C≡C-H), 2116(C≡C), 1628(C=O), 1592 (C=N), 1454 (CH_3-C), 1305 (CH_2-N), 1171, 1257 (O-CH_2), 972 (C-C).

1H NMR (25^{o}C, $CDCl_3$): δ (400 MHz) = 10.00 (s, 1H, -CH=N), 6.68-8.14 (m, 7H, Ar), 4.76 (d, 4H,-OCH_2-), 3.14(s, 3H,-NCH_3), 2.57 (t, 2H, -C≡CH), 2.49(s, 3H, -C-CH_3).

13C NMR ($CDCl_3$, 25^{o}C): δ (101 MHz) = 161.0, 160.3, 158.3, 151.6, 135.0, 129.0, 127.4, 126.6, 124.1, 121.2, 119.8, 107.4, 100.6, 78.3, 75.9, 56.2, 36.0, 10.1.

3. Calculated biological properties:

The introduction of single new drug into the market desires nearly 12 years and costs about billion dollars for execute this process. High cost, long time duration, high level of risk, highly complex procedures, uncertainty in the results, are the major threats in the growth of new drug. To defeat these difficulties, it is required to recruit cost effective drug designing method. Computer aided drug design are appraised to be substantial equipment for exploration of pharmacokinetic and pharmacodynamic properties. Proper execution of these methods could lead to a minimization in cost of drug designing and development. Molecular hybridization is an attractive strategy which based on the customizing of two different pharmacophores to fabricate hybrid molecules that can act as “double-edged swords”. It is considered that these molecules will impart marvellous activity with dual action that can control resistance[20, 21].

To maintain a pharmaceutically friendly profile, there is a rule called ‘Lipinski rule of five’; according to this rule, molecules must have molecular weights<500, clog P<5, H bond Donor <5 and H-bond acceptor <10. For a molecule to have good oral bioavailability, the number of rotatable bonds should be less than or equal to 10 and TPSA $\leq$ 140 Å, or sum of hydrogen bond donor and acceptor (HBD + HBA) should be ≤12. as assessed by Veber rule[22]. The synthesized compounds 3a-3h was examined for their physicochemical properties using Molinspiration software. Luckily in our case, all the synthesized compounds obey lipinski rule as well as Veber rule as summarized in table 1.

Table 1: In *silico* physicochemical properties of Antipyrine functionalized alkynes (3a-3h)

Comp. ID	M.W	cLog P	TPSA	nON	Nrotb	$N_{Violations}$
Lipinski rule	≤500	<5	<140	-	<15	<1
4-AAP	203	0.81	52.96	4	1	0
3a	345	3.03	48.54	5	5	0
3b	345	3.05	48.54	5	5	0
3c	345	3.08	48.54	5	5	0
3d	389	3.04	57.77	6	7	0
3e	375	2.84	57.77	6	6	0
3f	375	2.67	57.77	6	6	0
3g	395	4.19	48.54	5	5	0
3h	399	3.22	57.77	6	7	0
Metronidazole	171	-0.47	83.88	6	3	0

The activity score of kinase inhibitor, nuclear receptor ligand, protease inhibitor and enzyme inhibitor is calculated for synthesised compounds and shown in Table 2.

Table2: Comparative bioactivity of compounds (3a-3h) and reference drug (metronidazole)

Comp. id	GPCR	ICM	KI	NI	PI	EI
3a	-0.68	-1.15	-0.57	-0.77	-0.82	-0.44
3b	-0.7	-1.09	-0.58	-0.76	-0.86	-0.43
3c	-0.7	-1.08	-0.56	-0.76	-0.85	-0.43
3d	-0.69	-1.02	-0.56	-0.75	-0.84	-0.44
3e	-0.68	-1.12	-0.57	-0.81	-0.84	-0.46
3f	-0.69	-1.06	-0.54	-0.78	-0.86	-0.43
3g	-0.54	-0.94	-0.44	-0.66	-0.68	-0.33
3h	-0.6	-1.01	-0.51	-0.64	-0.72	-0.39
Met.	-1.09	-0.87	-0.59	-1.74	-1.68	-0.32

Pharmacokinetic Profile

PK is well described by ADMET[23-25], open source database, represents a number of stages occur when the drug come in contact with the organism.

All the synthesized acetylinic antipyrine derivatives were investigated through ADMET tool and it was revealed that all the compounds impart good pharmacokinetic profile. HIA values of the investigated compounds fall in the range of 97.39-99.84 thus displaying their excellent absorption behaviour. Caco-2 model revealed a similar value for bis acetylinic antipyrine (3h) as metronidazole however all other compounds shows good Caco-2 values falling in the range 39.39-57.65.MDCK cell model reveals a little lower value for 3f (0.316). As 3e has very low value of BBB which is almost similar to the reference drug while for other compounds it ranges between 0.205 - 0.628.Moreover 3b has excellent value than reference drug. All the compounds depict excellent binding to the plasma proteins. Skin permeability (log Kp) varies from-2.19 to -3.44. 3h exhibit eminent value for skin permeability among the synthesized compounds.

Table 3: Pharmacokinetic performance of anti pyrine functionalized compounds (3a-3h) and reference drug using ADMET web server

Com. ID	BBB	Buffer solubility	Caco2	HIA	MDCK	Plasma protein binding	Pure Water solubility	Skin per-meability	SKLog D	SKLog P
3a	0.182	0.166	39.39	97.54	115.14	89.85	10.72	-2.44	2.66	2.66
3b	0.628	0.177	58.23	97.40	42.33	92.07	8.09	-2.41	2.71	2.71
3c	0.061	0.297	41.89	97.40	42.33	93.62	7.68	-2.41	2.67	2.67
3d	0.069	0.083	56.18	97.39	1.76	92.21	3.37	-2.43	3.04	3.04
3e	0.449	0.103	57.17	97.42	80.57	89.58	9.60	-2.52	2.58	2.58
3f	0.205	0.167	57.65	97.42	0.316	92.27	5.440	-2.54	2.67	2.67
3g	0.187	0.010	47.23	97.81	12.64	90.83	0.216	-2.19	3.8	3.8
3h	0.140	0.044	21.73	99.84	1.27	89.05	2.05	-3.44	2.98	2.98
Met.	0.462	2.2938e+006	18.71	60.06	199.99	90.57	-	-2.65	-2.20	-0.64

3.2Biological Assay:
In vitro anti parasitic effect

Acetylinic antipyrine 3a-3h was assessed for their anti parasitic activities and results against parasitic strains are epitomized in Fig 2 and Fig 3. Various substituted aldehydes have been engaged to give a family of Schiff base linked antipyrine derivatives and reconnaissance their possibilities to curb the parasitic and bacterial infection. The screening results disclosed that the antipyrine acetylinic derivatives display majestic response on the anti parasitic potency. Against parasitic strains, antipyrine derivatives manifested curtailed activities compared to their activity against bacterial strains. The significant activity is shown by compound 3g with enhanced aromatic region against E. histolytica IC50 value of 10.65 µM at 24 hrs. while 3f (IC50=1.40 µM) is also found to show marvelous activity against the same strain at 48 hrs as shown in Fig2

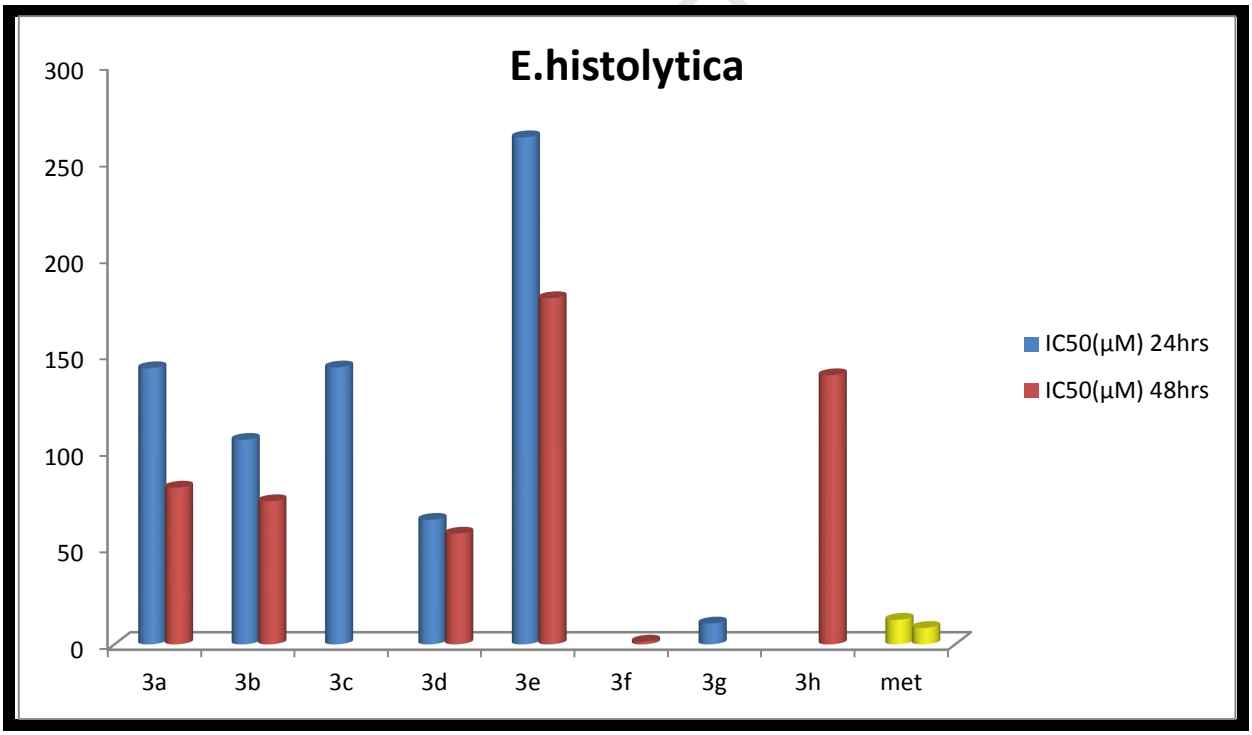

Fig 2: Anti parasitic activity of compounds (3a-3h) against E. histolytica at 24hrs. and 48 hrs.

Compounds 3b and 3g was displayed superior activity against G.lambia with IC_{50} values of 44.81, 16.89µM respectively. Moreover 3h manifested magnificent activity (IC50= 4.20µM)

as shown in Fig 3 which illustrate the presence of acetylinic framework. Drug efficacy is strongly dependent on time. The efficiency of all the synthesized compounds increased at 48hrs incubation as shown in Fig 3.

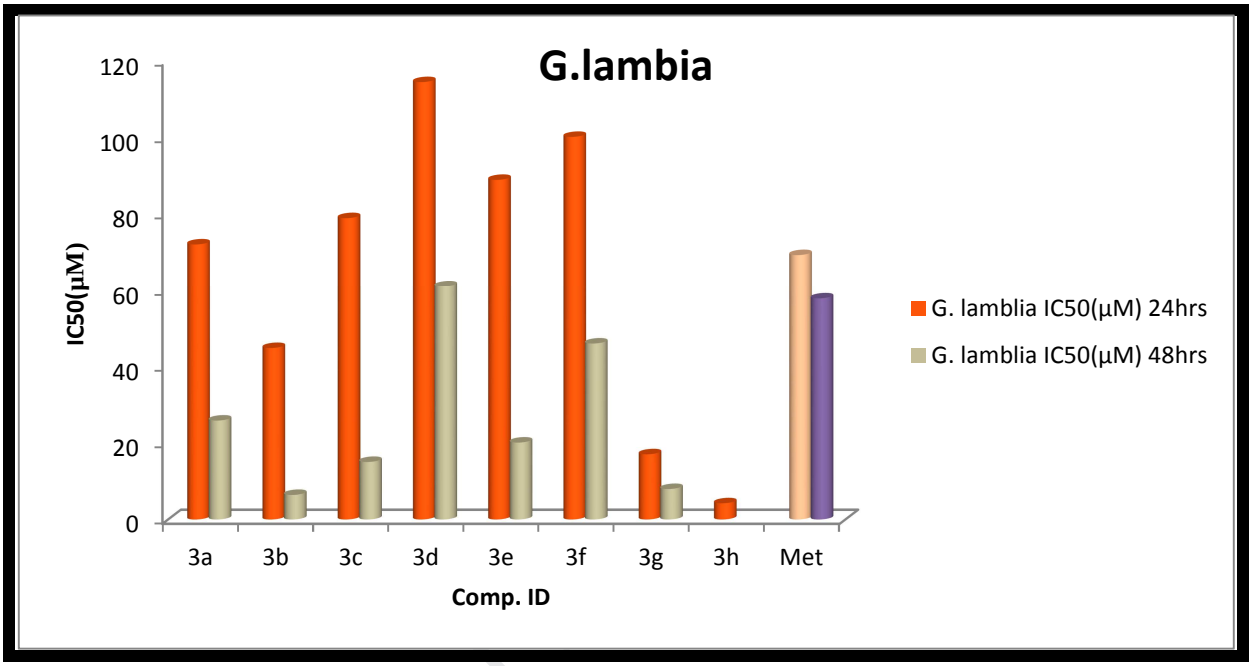

Fig 3: Anti parasitic activity of compounds(3a-3h) against G. lambia at 24hrs. and 48 hrs.

Antimicrobial activity

The antibacterial activity was categorized as highly active (>14 mm), moderately active (10-14 mm) and slightly active (6-10 mm) and less than 5 mm was taken as inactive[26]. It is revealed from table that 3b, 3c, 3d, 3e, 3h antipyrine acetylinic derivatives exhibit moderate activity as shown in table 4.

Table 4: Zone of inhibition (mm) of compounds (3a-3h) against various bacterial strain

Sr.no.	**Staphylococcus aureus**	**Bacillus subtillus**	**Vibrio cholera**	**E.coli**
3a	-	-	-	-
3b	9	-	-	9
3c	11	-	9	-
3d	-	-	9	-
3e		9	9	9
3f	-	-	-	-

3g	-	-	-	-
3h	-	9	9	-

compounds 3c with acetylinic group at para position are found to be the most potent against S. aureus. Bis Acetylinic antipyrine 3h is the most effective ones against E. coli bacterial strain with IC50 value of 0.29 mM. The significant activity is shown by compound 3h which is a bis-acetylinic compound with IC50 value of 0.32 mM against Bacillus subtillus strain and 0.3 mM for vibrio cholera. Acetylinic antipyrine 3e with methoxy group displayed dignified potency with IC50 value of 0.33 mM against Bacillus subtillus and 0.31mM against vibrio cholera as shown in Fig 4.

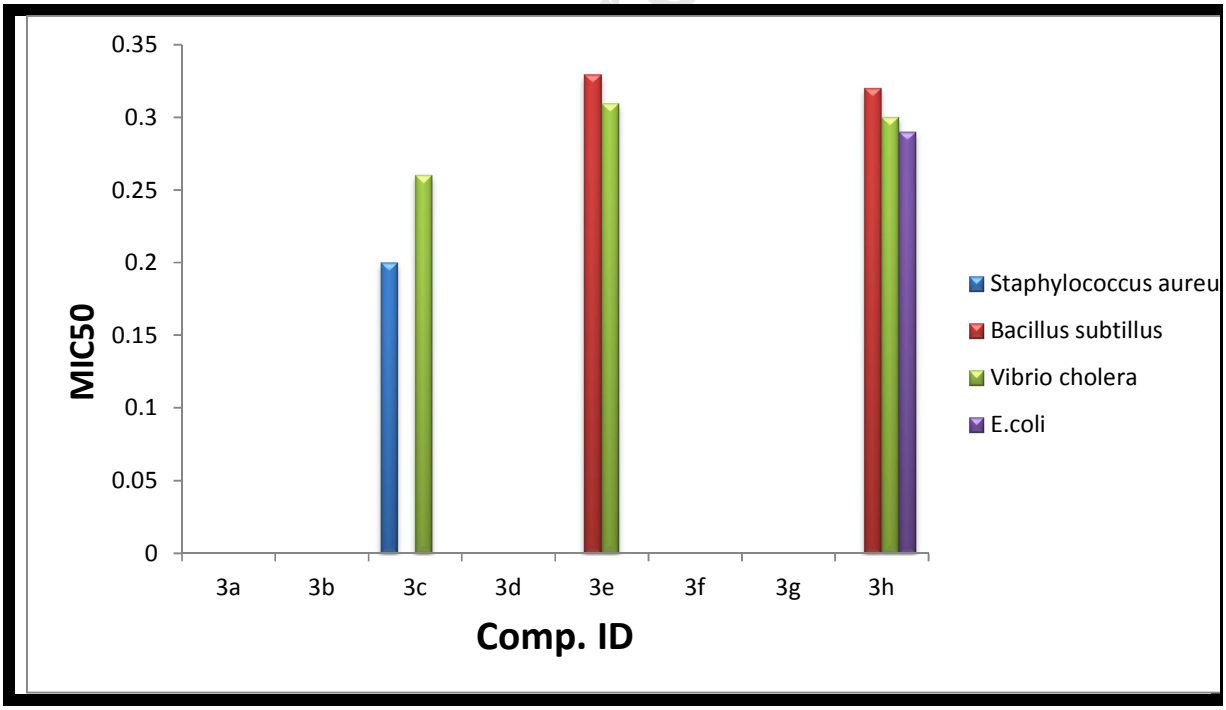

Fig 4: In vitro antibacterial activity of compounds (3a-3h) against bacterial strains of using microbroth dilution assay (MDA)

4. Result and Discussion:

4.1 Spectroscopic analyses

IR spectra

IR spectra of compounds displayed a stretching band at 1628–1648 cm^{-1} that assigned to antipyrine ν (C=O) stretching vibrations of carbonyl bond. Since frequency of carbonyl group appears at 1700 cm^{-1} around but due to conjugation in the ring, this appears in the region 1628-1648 cm^{-1}. The band around 2100 $cm^{-1}$and 3300 cm^{-1} in antipyrine functionalized alkyne **3a-3h** confirms the formation of C≡C and C≡CH respectively. Moreover, stretching vibrations of –C=N appear in the range of 1570-1600 cm^{-1} .

NMR spectra

In the 1H spectra of all compounds, a singlet in the region δ = 9.73–10.45 ppm assigned to imine proton. Alkynyl proton (C≡C**H**) for 3a–3h appears around δ = 2.40–2.60 ppm, OCH2 proton which linked to alkynyl group appear as doublet at 4.75-4.92 ppm. The aromatic ring protons were appeared as multiplets in the region δ~ 8.87–6.74 ppm. Moreover, in case of 3e and 3f, the $–OCH_3$ protons displayed as singlet in the region δ~3.90 and 3.94 ppm respectively.

In ^{13}C NMR spectra, for carbonyl carbon appears in the region δ ~ 161.3 ppm due conjugation within the pyrazole ring and spectra of all other compounds, the aromatic carbon displayed in the region δ ~ 158.2-120.0 ppm. Two carbons of alkynyl moiety **3a-3h** observed in the range of δ ~ 72.1-77.2ppm. Two methyl carbon allied to pyrazole ring appear at δ ~ 10.0 and 36.0 (attached to nitrogen).

4.2. X-ray structure determination

Sr.no	Crystal Structure	Lattice arrangement

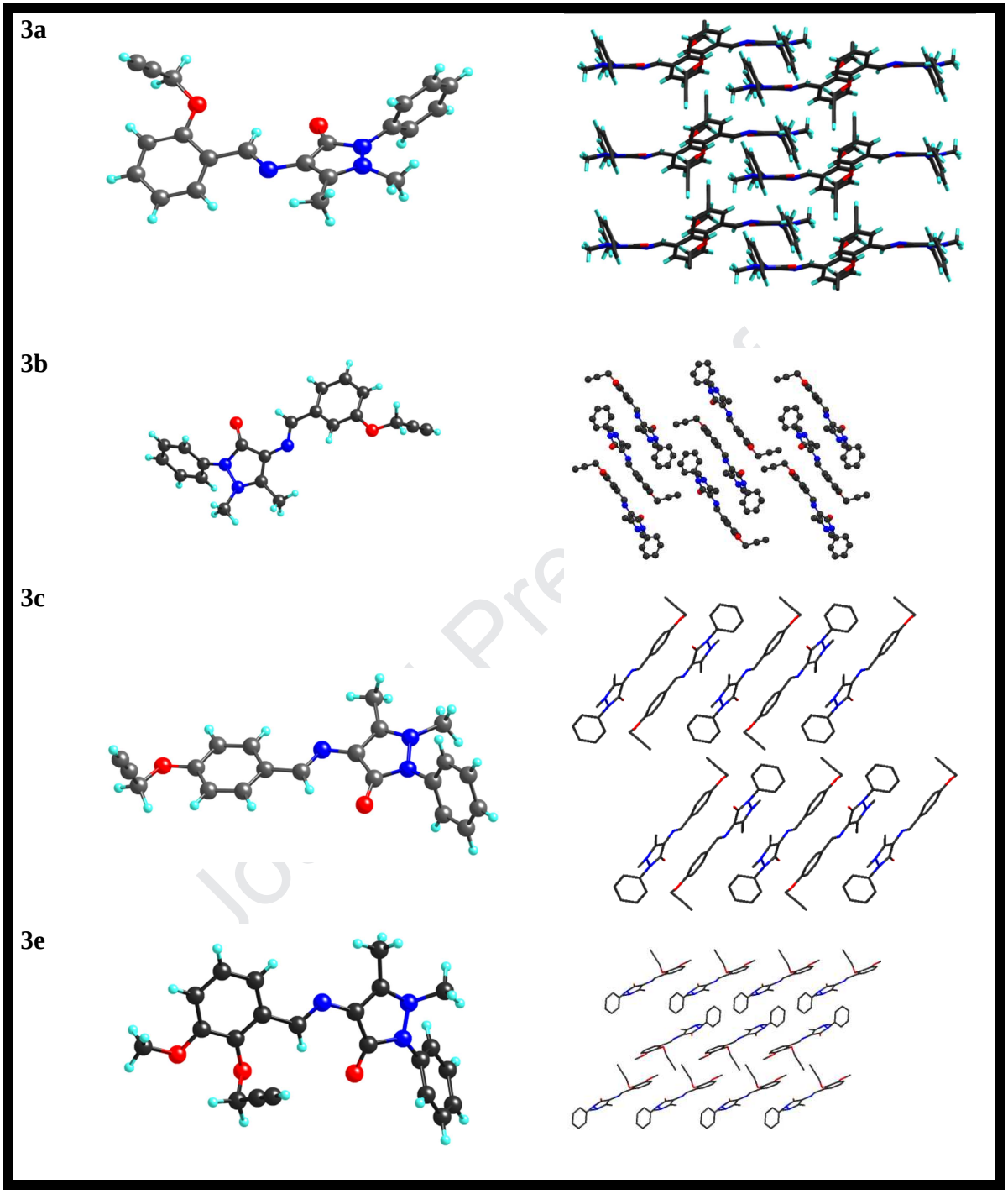
3a
3b
3c
3e

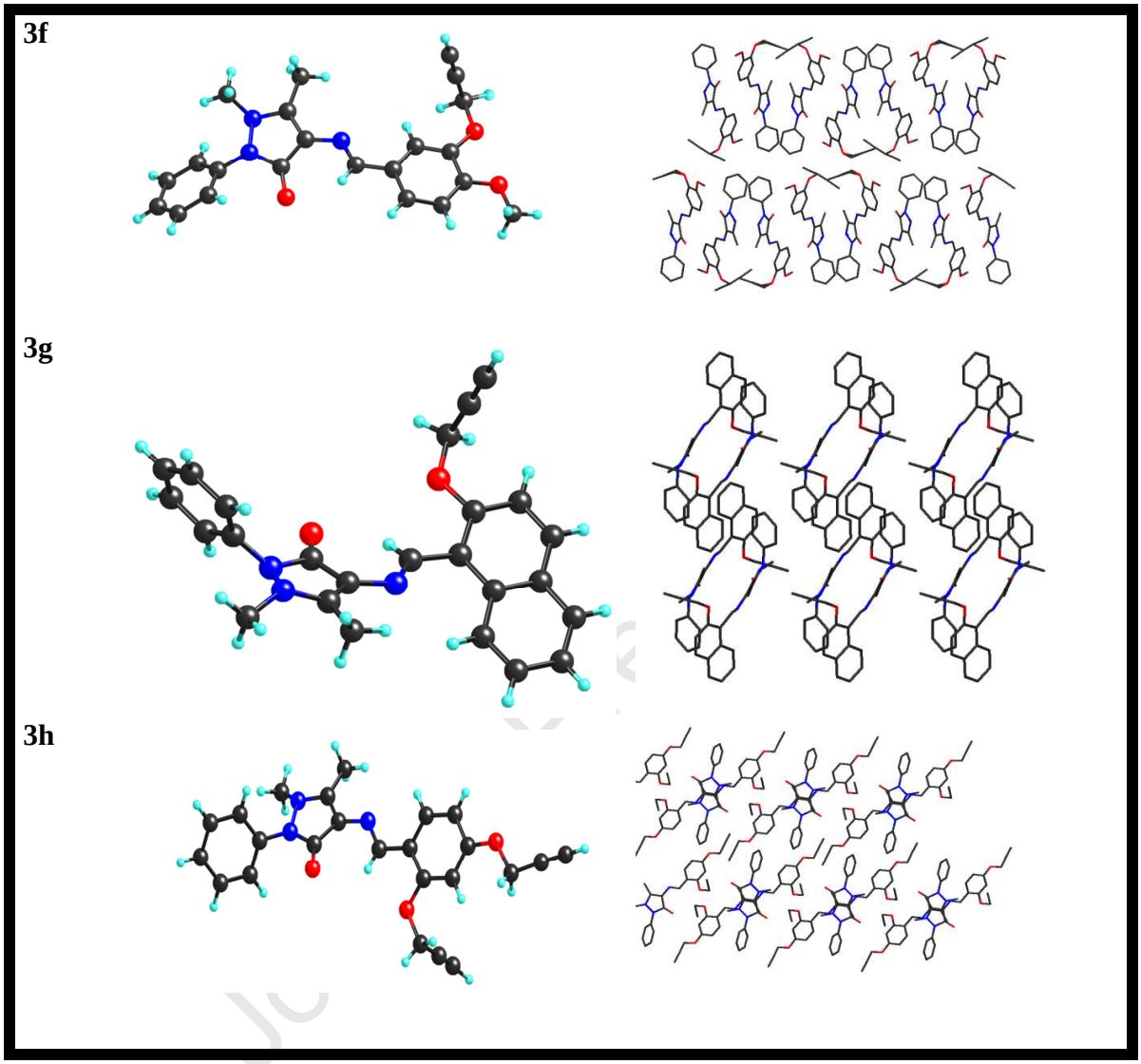

Fig 5: Ball and stick diagram of molecule 3a, 3b, 3c, 3e, 3f, 3g, 3h with colour code as grey: C, red: oxygen, Blue: Nitrogen, and sky blue: hydrogen and their lattice arrangement.

The molecule **3a** crystalizes in triclinic P-1 space group. The asymmetric unit contain one molecule per unit cell. The central pyrazolidin moiety along with aromatic group's forms planar arrangement with a perpendicular position to the acetylene ether group. Two types of weak interactions of C–H···O and π··π interactions facilities the formation a small cavity like arrangement favouringπ··π interactions between two aromatic groups along *bc*-plane. The molecule **3b** has almost similar framework structureand only differs by the position of acetylene ether group at meta position as compared to ortho position for **3a**. The molecule **3b** crystalizes in P 2_1/n space group of monoclinic system. The asymmetric unit contain one

molecule per unit cell. The central pyrazolidin moiety along with aromatic group's forms planar arrangement with a perpendicular position to the acetylene ether group. Two weak interactions of C−H···O type between carbonyl group (O) of pyrazolidn and H-atoms of arromatic and CH_2 group helps a head-tail alignment along *ac*-plane and with an overall layer like arrangement. The molecule **3c** crystalizes in triclinic P-1 space group. The asymmetric unit contain one molecule per unit cell. The central pyrazolidin moiety along with aromatic group's forms planar arrangement with a perpendicular position to the acetylene ether group. In the lattice arrangement there is no strong H-bonds however, the weak interactions of C−H···O type between carbonyl group (O) of pyrazolidn and H-atoms of arromatic and CH2 group favours a head-tail alignment along bc-plane and with an overall zig-zag arrangement. The molecule **3e** has an additional methyl ether group attached ortho position to the acetylene ether group as compared to **3a** and **3b**. The molecule **3e** crystalizes in P 2_1/c space group of monoclinic system. The asymmetric unit contain one molecule per unit cell. Weak interactions of C−H···O, C−H··π type favours layer like alignment along *ac*-plane where all acetylene ether group part of one layer and aromatic units of other layer. The molecule **3f** has almost similar structure with that of **3e** and only differ by the position of ether groups i.e at meta and para positions as compared to **3e**. The molecule **3f** crystalizes in P 2_1/c space group of monoclinic system. The asymmetric unit contain two molecules per unit cell. Weak interactions of C−H···O, C−H··π type favours layer like alignment along *bc*-plane where two molecules are cluster together either in their un-substituted aromatic (head) end or ether substituted end (tail) position. The molecule **3g** has a naphthalene group attached with an acetylene ether moiety at ortho position as compared to **3a** and **3b**. The molecule **3g** crystalizes in P -1 space group of triclinic system. The asymmetric unit contain one molecule per unit cell. Only one weak interactions of C−H··π type favours layer ribbon like alignment along *ac*-plane. The molecule **3h** has a similar structural framework as **3e** where the two substituents are acetylene ether type moiety at meta position to each other. The molecule **3h** crystalizes in I2/a space group of monoclinic system. The asymmetric unit contain one molecule per unit cell. One of the acetylene group anchoring perpendicular to aromatic ring to form a weak interactions of C−H··π (3.665 (3) Å and forms discreet 0D lattice structure along *ac*-plane.

Table 5: Crystallographic Data and Refinement Parameters for the molecules (3a,3b,3c)

Complexes	**3a**	**3b**	**3c**
CCDC	1860156	1860155	1860153
Empirical formula	C21 H19 N3 O2	C21 H19 N3 O2	C21 H19 N3 O2
M_r [g mol^{-1}]	345.40	345.40	345.40
T (K)	293(2)	293(2)	293(2)
wavelength (A°)	0.71073	0.71073	0.71073
crystal system	Triclinic	Monoclinic	Triclinic
space group	*P*-1	*P121/n1*	*P*-1
a [Å]	7.1765(9)	11.1873(8)	6.9967(1)
b [Å]	11.1338(9)	.2144(4)	9.7597(2)
c [Å]	11.9194(15)	23.3211(13)	14.0933(3)
α [deg]	77.363(9)	90	74.729(2)
β [deg]	78.259(11)	98.036(6)	82.583(2)
γ [deg]	77.683(9)	90	82.153(2)
V [$Å^3$]	895.55(18)	1863.8(2)	915.32(3)
Z	2	4	2
ρ_{calc}[g cm^{-3}]	1.280	1.230	1.253
μ [mm^{-1}]	0.084	0.081	0.082
F (000)	364.2	728.3	364.2
crystal size $[mm]^3$	0.33 × 0.22 × 0.2	0.31 × 0.26 × 0.19	0.30 × 0.23 × 0.15
reflection collected	9657	13198	12358
independent reflections	3340	3872	3878
GOF on F^2	1.0565	1.11	1.0188
final R indices(R1/wR2) [I > 2σ(I)]	0.0473/ 0.1157	0.0692/ 0.2298	0.0476/ 0.1233
R indices (R1/wR2) all data	0.0655/ 0.1287	0.1128/ 0.3118	0.0653/ 0.1358

Table 6: Crystallographic Data and Refinement Parameters for the molecules (3e, 3f, 3g, 3h).

Complexes	**3e**	**3f**	**3g**	**3h**
CCDC	1860154	1860159	1860157	1860158
Empirical formula	C22 H21 N3 O3	C44 H37.5 N6 O6	C25 H21 N3 O2	C24 H21 N3 O3
M_r [g mol^{-1}]	375.43	746.32	395.46	399.45
T (K)	293(2)	99(3)	99(3)	99(3)
wavelength (A°)	0.71073	1.54184	1.54184	1.54184
crystal system	Monoclinic	Monoclinic	Triclinic	Monoclinic
space group	*P121/c1*	*P121/c1*	*P*-1	*I12/a1*
a [Å]	15.7933(7)	7.5275(3)	9.4115(2)	22.6184(10)
b [Å]	7.4190(3)	18.6777(12)	10.1999(2)	7.4281(3)

c [Å]	17.0451(6)	27.8013(11)	11.5282(3)	27.2477(12)
α [deg]	90	90	69.240(2)	90
β [deg]	106.103(4)	95.385(4)	84.099(2)	113.106(5)
γ [deg]	90	90	83.363(2)	90
V [Å^3]	1918.82(14)	3891.5(3)	1025.60(4)	4210.7(4)
Z	4	4	2	8
ρ_{calc}[g cm^{-3}]	1.299	1.2738	1.2805	1.2601
μ [mm^{-1}]	0.088	0.087	0.083	0.085
F (000)	792.4	1566.8	416.2	1566.8
crystal size [mm]^3		0.25 × 0.15 × 0.15	0.28 × 0.16 × 0.14	0.27 × 0.20 × 0.18
reflection collected	15442	11735	14001	16900
independent reflections	4083	5097	4354	4461
GOF on F^2	1.0010	1.0429	1.0424	1.0166
final R indices(R1/wR2) [I > 2σ(I)]	0.0548/ 0.1320	0.0683/ 0.1796	0.0447/ 0.1115	0.0556/ 0.1522
R indices (R1/wR2) all data	0.0814/ 0.1490	0.0997/ 0.2036	0.0673/ 0.1246	0.0861/ 0.1765

Table 7: Selected Bond Lengths (Å) and bond angles (˚) for the molecules (3a, 3b, 3c, 3e, 3f, 3g, & 3h)

Compound 3a	Length/Å		Length/Å		Length/Å
O23 C6	1.3684(19)	C12 C11	1.366(2)	N9 N13	1.3966(18)
O23 C24	1.432(2)	C12 C22	1.485(2)	N9 C14	1.424(2)
O20 C10	1.2411(18)	C11 C10	1.437(2)	N9 C10	1.385(2)
N8 C11	1.398(2)	C14 C15	1.376(3)	N13 C12	1.3498(19)
N8 C7	1.280(2)	O23 C6	1.3684(19)	N13 C21	1.446(2)
N9 N13	1.3966(18)	O23 C24	1.432(2)	N13 C21	1.446(2)
N9 C14	1.424(2)	O20 C10	1.2411(18)	N8 C7	1.280(2)
N9 C10	1.385(2)	N8 C11	1.398(2)	N13 C12	1.3498(19)
C24 O23 C6	118.63(13)	C2 C1 C6	118.04(15)		
	Angle/˚		Angle/˚		Angle/˚
C7 N8 C11	120.14(13)	C1 C7 N8	120.70(15)	C11 C10 N9	104.53(14)
C14 N9 N13	120.28(14)	C1 C6 O23	115.44(14)	C16 C15 C14	119.20(18)
C10 N9 N13	109.66(12)	C5 C6 O23	124.02(16)	C21 N13 C12	127.15(13)
C10 N9 C14	125.89(13)	C5 C6 C1	120.54(16)	C11 C12 N13	109.73(13)
C12 N13 N9	107.32(13)	N9C10 O20	123.65(14)	C11 C10 O20	131.82(16)
C21 N13 N9	120.47(13)				

[i]-X,-X+Y,-Z

Compound 3b	Length/Å		Length/Å		Length/Å
O20 C13	1.239(3)	N9 C14	1.420(3)	C14 C19	1.376(4)
O23 C3	1.379(4	N10 C11	1.352(3)	C11 C22	1.487(4)
O23 C24	1.415(4)	N10 C21	1.443(3)	C14 C15	1.387(4)
N8 C12	1.381(3	C13 C12	1.445(4)	N9 N10	1.410(3)
N8 C7	1.279(3)	C12 C11	1.373(4)	N9 C13	1.393(3)
	Angle/˚		Angle/˚		Angle/˚
C24 O23 C3	118.9(3)	C11 C12 N8	122.3(2)	C12 C13 O20	131.6(2)
C7 N8 C12	122.1(2)	C11 C12 C13	107.4(2)	C12 C13 N9	105.2(2)
C13 N9 N10	109.1(2)	C12 C11 N10	110.6(2)	C13 C12 N8	130.2(2)
C14 N9 N10	120.1(2)	C22 C11 N10	121.8(2)	C11 N10 N9	107.1(2)
C14 N9 C13	123.5(2)	N9 C13 O20	123.2(2)	C21 N10 N9	118.7(2)
C21 N10 C11	126.2(2)				
Compound 3c	Length/Å		Length/Å		Length/Å
O20 C10	1.2401(16)	C1 C6	1.386(2)	C19 C18	1.379(3)
O23C4	1.3749(18)	C12 C22	1.4857(19)	C15 C16	1.367(3)
O23 C24	1.4256(19)	C2 C3	1.368(2)	C18 C17	1.374(3)
N8 C11	1.3938(18)	C4 C5	1.379(2)	C17 C16	1.360(3)
N8 C7	1.2763(18)	C4 C3	1.385(2)	C14 C15	1.378(2)
N9 N13	1.3916(16)	C14 C19	1.373(2)	C6 C5	1.381(2)
N9 C10	1.3914(18)	C11 C10	1.433(2)	C24 C25	1.446(3)
N9 C14	1.4173(19)	C1 C2	1.394(2)	C25 C26	1.157(3)
N13 C12	1.3471(19)	C1 C7	1.458(2)	C11 C12	1.37(2)
N13 C21	1.4507(19)				
	Angle/˚		Angle/˚		Angle/˚
C24 O23 C4	118.25(12)	C11 C10 N9	104.89(11)	C15 C14 N9	120.90(15)
C7 N8 C11	120.19(13)	C3 C2 C1	121.30(14)	C15 C14 C19	120.68(16)
C10 N9 N13	109.47(12)	C1 C7 N8	122.15(14)	C5 C6 C1	122.18(14)
C14 N9 N13	122.09(12)	C5 C4 O23	125.00(14)	C6 C5 C4	119.00(14)
C14 N9 C10	124.13(12)	C3 C4 O23	114.96(13)	C4 C3 C2	120.17(14)
C12 N13 N9	107.61(11)	C3 C4 C5	119.99(14)	C25 C24 O23	112.18(14)
C21 N13 N9	121.04(13)	C19 C14 N9	118.39(15)	C26 C25 C24	177.4(2)
C21 N13 C12	128.37(13)	C22 C12 N13	121.68(13)	C18 C19 C14	119.27(19)
C12 C11 N8	122.33(13)	C22 C12 C11	128.36(14)	C16 C15 C14	119.2(2)
C10 C11 N8	129.87(12)	N9 C10 O20	122.65(13)	C17 C18 C19	119.8(2)
Compound 3e	Length/Å		Length/Å		Length/Å
O23 C6	1.381(2)	C11 C12	1.364(2)	C6 C1	1.391(2)

O23 C24	1.440(2)	C14 C15	1.377(2)	C6 C5	1.404(2)
O20 C10	1.230(2)	C14 C19	1.385(3)	C1 C7	1.463(2)
O27 C5	1.359(2)	C5 C4	1.382(3)	C1 C2	1.398(3)
O27 C28	1.426(2)	C15 H15	0.9300	C10 C11	1.435(2
N9 N13	1.404(2)	C15 C16	1.376(3)	C7 H7	0.9300
N9 C10	1.404(2)	N8 C11	1.396(2)	N13 C12	1.366(2)
N9 C14	1.418(2)	N8 C7	1.278(2)	N13 C21	1.462(2)
	Angle/˚		Angle/˚		Angle/˚
C24 O23 C6	117.43(14)	N9 C10 O20	123.17(16)	C21 N13 N9	117.83(14)
C28 O27 C5	117.24(17)	C11 C10 O20	132.03(16)	C21 N13 C12	123.80(16)
C10 N9 N13	109.08(14)	C11 C10 N9	104.76(15)	C1 C6 O23	118.21(15)
C14 N9 N13	120.06(14)	C1 C7 N8	120.55(17)	C7 C1 C6	120.03(16)
C14 N9 C10	122.65(15)	C5 C6 O23	120.75(16)	C2 C1 C6	118.83(16)
C11 N8 C7	120.87(16)	C5 C6 C1	120.79(16)	C2 C1 C7	121.14(16)
C12 N13 N9	107.09(13)				
Compound 3g	Length/Å		Length/Å		Length/Å
O24 C14	1.2351(16)	O24 C14	1.2351(16)	N17 C16	1.3579(18)
O27 C2	1.3751(17)	O27 C2	1.3751(17)	N17 C25	1.4514(19)
O27 C28	1.4279(18)	O27 C28	1.4279(18)	C15 C16	1.3669(19)
N13 N17	1.4013(16)	N13 N17	1.4013(16)	C15 C14	1.4378(19)
N13 C14	1.4027(18	N13 C14	1.4027(18)	C16 C26	1.482(2)
N13 C18	1.4315(18)	N13 C18	1.4315(18)	C1 C11	1.4654(19)
N12 C15	1.4006(17)	N12 C15	1.4006(17)	C1 C10	1.4266(19)
N12 C11	1.2789(17)	C1 C2	1.384(2)		
	Angle/˚		Angle/˚		Angle/˚
C28 O27 C2	119.40(12)	C16 C15 N12	123.29(13)	C16 N17 N13	107.38(11)
C14 N13 N17	108.59(11)	C14 C15 N12	128.79(12)	C25 N17 N13	117.96(12)
C18 N13 N17	119.12(11)	C14 C15 C16	107.66(12)	C25 N17 C16	125.60(13)
C18 N13 C14	120.95(12)	C15 C16 N17	110.31(12)	C26 C16 C15	128.34(14)
C11 N12 C15	118.31(12)	C26 C16 N17	121.34(13)	C2 C1 C10	118.88(13)
C10 C1 C11	124.98(13)	C19 C18 C23	120.77(15)	C1 C11 N12	124.04(13)
C2 C1 C11	116.12(12)	C23 C18 N13	120.62(14)	C19 C18 N13	118.51(14)
Compound 3h	Length/Å		Length/Å		Length/Å
O001 C007	1.3683(19)	N006 C009	1.420(2)	N004 C008	1.349(2)
O001 C00B	1.4222(19)	N006 C00E	1.383(2)	N004 C00K	1.456(2)
O002 C00E	1.239(2)	C007 C00G	1.389(2)	N005 C00C	1.279(2)
O003 C00F	1.365(2)	C007 C00H	1.397(2)	N005 C00D	1.393(2)
O003 C00O	1.428(2)	C008 C00D	1.368(2)	C008 C00N	1.482(2)
N004 N006	1.3975(19)	C009 C00L	1.378(2)		
	Angle/˚		Angle/˚		Angle/˚
C0B O01 C07	118.90(13)	C0L C09 N06	120.45(16)	C0D C08 N04	109.99(15)
C0O O03 C0F	117.99(14)	C0M C09 N06	119.61(16)	C0N C08 N04	122.09(16)
C08 N04 N06	106.99(13)	C0M C09 C0L	119.93(18)	C0N C08 C0D	127.80(17)

C0K N04 N06	118.75(14)	C0B O01 C07	118.90(13)	C0G C07 O01	123.12(15)
C0K N04 C08	124.93(14)	C0O O03 C0F	117.99(14)	C0H C07 O01	115.48(14)
C0D N05 C0C	120.84(15)	C0E N06 N04	110.11(14)	C0H C07 C0G	121.40(16)
C09 N06 N04	120.48(13)	C0E N06 C09	127.33(15)		

5. Conclusion and Future Prospects:

In Summary, We have outline a unified strategy for fabricate tangible green drug. These drug candidates were selected by primary screenings and further subjected to in vitro anti-bacterial as well as anti parasitic activities comparable or even superior to those of approved drugs like metronidazole. This study sheds light on biological activity of anti pyrine derivatives and promotes further research for bio-medical applications. In the long term, such materials will endorse further research in developing new channels for the medication of infectious diseases.

Acknowledgements

We thankfully acknowledge receipt of financial support from the Department of Science and Technology, New Delhi, India through the scheme DST SERB, DST-PURSE II , CSIR and DST FIST (X-ray Crystallography).One of the author Pinky Satija would like to thank DST for Inspire Fellowship in the form of SRF.

Conflict of Interest

There are no conflicts to declare.

Supplementary appendix

CCDC- 1860156 (**3a**), 1860155 (**3b**), 1860153 (**3c**), 1860154 (**3e**), 1860159 (**3f**), 1860157 (**3g**), 1860158 (**3h**) contain the supplementary crystallographic data for this paper. These data can be obtained free of charge from the Cambridge Crystallographic Data Centre via www.ccdc.cam.ac.uk.

List of abbreviation :

AAP - Amino antipyrine

Met - Metronidazole

MW - Microwave

G.lambia - Giardia lambia

E.histolytica - Entamoeba histolytica

Naph- Naphthalene

References:

1. M. B. Gawande, S. N. Shelke, R. Zboril, R. S. Varma, Acc. Chem. Res 47(2014) 1338−1348.
2. R. Karu, S.Gedu, Green Chem., 20(2018) 369-374.
3. N. Uramaru, H. Shigematsu, A. Toda, R. Eyanagi, S. Kitamura, S. Ohta, J. Med. Chem 53(2010) 8727–8733.
4. V. Jaiswal, Kalyani, R. B. Rastogi, Rajesh Kumar, J. Mater. Chem. A 2(2014)10424.
5. F. Mahle , T. da Rosa Guimarães , A. Vergilina Meira , R. Corrêa , R. Cé Bella Cruz , A. Bella Cruz , R. José Nunes , V. Cechinel-Filho, F. de Campos-Buzzi, EJMC 45(2010) 4761- 4768.
6. C. Remes , A. Paun , I. Zarafu , M. Tudose , M.T. Caproiu , G. Ionita , C. Bleotu , L. Matei, P. Ionita, Bioorganic Chemistry 41(2012) 6–12.
7. G. Singh, P. Kalra, A. Arora, A. Singh, G. Sharma, Sanchita, I. K. Maurya, S. Dutta, P. Munshi, V. Verma. Chemistry Select *3(*2018) 2366– 2375
8. Y. Hu, Y. Shen, X. Wu, X. Tu and G.-Xue Wang. EJMC 143(2018) 958-969.
9. P. Teng, A. Nimmagadda, M. Su, Y. Hong, N. Shen, C. Li, L.-Yu Tsai, J. Cao, Q. Li, J. Cai. Chem. Commun**.** 53(2017) 11948.
10. S. Singh, N. Bharti, P. P. Mohapatra. Chem. Rev. 109**(**2009**)** 1900–1947.
11. C. Bustos-Brito, M. Sánchez-Castellanos, B. Esquivel, J. S. Calderón, F. Calzada, L.Yepez-Mulia, A. Hernández-Barragán, P. Joseph-Nathan, G. Cuevas, L. Quijano. J. Nat. Prod. 77(2014) 358−363.
12. G. Singh, P. Satija, A.Singh, Sanchita, D. Aulakh, M. Wriedt, C. E. Ruiz, M. A. Esteban, S. Sinha, R. Sehgal, Appl Organometal Chem. e4695(2019) 1-15.
13. D. E. Bosch, D. P. Siderovski. Biochemistry 54(2015) 404−412.
14. G.-Fu Zhang, X. Liu, S. Zhang, B. Pan, M.-Liang Liu. EJMC 146**(**2018**)** 599-612.

15. M. Y. Wani, A. Roouf Bhat, A. Azam, F. Athar, A. J. F. N. Sobral . Med. Chem. Commun., 7(2016) 982-989.
16. X. Li, B. Wu, H.Chen, K. Nan, Y. Jin, L. Sun, B.Wang, J. Mater. Chem. B 6(2018) 4274-4292.
17. Dolomanov, O. V, Bourhis, L. J., Gildea, R. J, Howard, J. A. K, Puschmann, H. *OLEX2*: a complete structure solution, refinement and analysis program. J. Appl. Cryst, *42(*2009) 339–341.
17.Burla, M. C, Caliandro, R, Camalli, M, Carrozzini, B Cascarano, G. L. De Caro, L. Giacovazzo, C. Polidori, G. Siliqi, D. Spagna, R. *IL MILIONE*: a suite of computer programs for crystal structure solution of proteins. J. Appl. Cryst *40(*2007) 609–613.
18. Sheldrick, G. M. Crystal structure refinement with *SHELXL*.ActaCryst, *C71 (*2015) 3–8.
19. M.A.Khanfar, D. Reiner, S tefan Hagenow, H. Stark, Bioorganic & Medicinal Chemistry. https://doi.org/10.1016/j.bmc.2018.06.028.
20. G. Singh, A. Arora , S. S. Mangat , S. Rani, H. Kaur, K. Goyal, R. Sehgal , I. K. Maurya ,R. Tewari , D. C.-Lazarte , S. Sahoo, Navneet Kaur. EJMC, 108(2016) 287-300.
21. G. Sliwoski, S.K. Kothiwale, J. Meiler, E. W. Lowe, Jr. Computational Methods in Drug DiscoveryPharmacol Rev. 66(2014) 334–395.
22. PreADMET program, 2004. Available from: URL: http://preadmet.bmdrc.org.
23. G. Singh, K. Chowdhary, P. Satija, A. Singh, B. Singh, K. Singh, C. Espinosa, M. A. Esteban, R. Sehgal, V. Verma, Chemistry Select *3(*2018) 1609– 1614.
24. G. Singh, A. Arora, A. Singh, P. Kalra, S. Rani, K. Singh, I. K. Maurya, R. S. Mandal, Chemistry Select 3(2018)1942– 1952.
25. G.Singh, S.Rani, S.Gawri, S. Sinha, R. Sehgal, NJC, *41(2017)11626-11639.*
26. G. Singh, S. Girdhar, A. Saroa, S. Girdhar, B.Singh, Phosphorus Sulfur and Silicon and the Related Elements DOI: 10.1080/10426507.2013.844145.

Research highlights:

- By using microwave methodology, a family of Anti pyrine derivatives were synthesized. This is an amazing quote of stitching anti pyrine nucleus to acetylene moiety.
- The protocol afforded the excellent yield in short span of time under eco friendly conditions.
- All the synthesized compounds are characterized by IR, NMR (^{1}H, ^{13}C), and Single X-ray diffraction.
- The hybrid molecules screened for their physicochemical properties using mol inspiration software and ADMET web server.
- This work articulates a new possible scaffold for drug discovery against protozoal pathogens (Entamoeba histolytica and Giardia lamblia) and bacterial strain (Staphylococcus aureus, Vibrio cholera E.coli, Bacillus subtillus) and this low price, versatile drug is hopefully leads to eventual elimination of parasitic disease from human population.